

Co-trading networks for modeling dynamic interdependency structures and estimating high-dimensional covariances in US equity markets

Yutong Lu¹, Gesine Reinert^{1,3}, and Mihai Cucuringu^{1,2,3,4}

¹Department of Statistics, University of Oxford, Oxford, UK

²Mathematical Institute, University of Oxford, Oxford, UK

³The Alan Turing Institute, London, UK

⁴Oxford-Man Institute of Quantitative Finance, University of Oxford, Oxford, UK

May 14, 2024

Abstract

The time proximity of trades across stocks reveals interesting topological structures of the equity market in the United States. In this article, we investigate how such concurrent cross-stock trading behaviors, which we denote as *co-trading*, shape the market structures and affect stock price co-movements. By leveraging a co-trading-based pairwise similarity measure, we propose a novel method to construct dynamic networks of stocks. Our empirical studies employ high-frequency limit order book data from 2017-01-03 to 2019-12-09. By applying spectral clustering on co-trading networks, we uncover economically meaningful clusters of stocks. Beyond the static Global Industry Classification Standard (GICS) sectors, our data-driven clusters capture the time evolution of the dependency among stocks. Furthermore, we demonstrate statistically significant positive relations between low-latency co-trading and return covariance. With the aid of co-trading networks, we develop a robust estimator for high-dimensional covariance matrices, which yields superior economic value on portfolio allocation. The mean-variance portfolios based on our covariance estimates achieve both lower volatility and higher Sharpe ratios than standard benchmarks.

Keywords: Market microstructure; Co-occurrence analysis; Network analysis; Machine learning; Robust covariance estimation; Portfolio allocation

1 Introduction

The pioneering work of Kyle (1985) posits that the price formation at high-frequency level is the result of the interplay among market participants. In this model, market makers monitor the aggregated order flows after informed and liquidity traders submit their orders, and then set their fair prices. With the development and boom of high-frequency trading (HFT) strategies, the interplay becomes more aggressive and sophisticated. Previous works (Brunnermeier and Pedersen (2005); Van Kervel and Menkveld (2019); Hirschey (2021); Yang and Zhu (2020); Goldstein, Kwan, and Philip (2023)) find that some HFT traders actively detect activities of other participants in the market, and fiercely trade against them. Furthermore, these interactions can span across different stocks (Hasbrouck and Seppi (2001); Bernhardt and Taub (2008); Capponi and Cont (2020)). We investigate concurrent (almost instantaneous) trading across multiple stocks, a phenomenon which we refer to as *co-trading* behavior, at a very granular level by directly considering individual trades, and zooming-in around their local neighborhoods.

In this paper, we propose a novel method that constructs *co-trading networks*, in order to model the complex structures of co-trading activities in equity markets. Constructed from limit

order books, our co-trading networks bridge the trading behaviors at a granular level with the dynamic topological structures of the equity market and price co-movements among individual stocks. Moreover, by making use of co-trading networks, we develop a robust estimator for high-dimensional covariance matrices, and demonstrate its conspicuous economic value on portfolio allocation.

The network construction starts with a pairwise similarity measure between stocks. Inspired by the idea of trade co-occurrence originating from Lu, Reinert, and Cucuringu (2022), we define the pairwise similarity as the normalized count of times that trades, for a given pair of stocks, arrive concurrently. We name this measure as a *co-trading score*, since it embeds the intuition that stocks frequently traded together are closely related. Concatenating co-trading scores between every pair of stocks, we obtain the co-trading matrix, which serves as the adjacency matrix of the proposed weighted network of equity markets.

Employing algorithms and tools for network analysis (Hagberg, Swart, and S Chult (2008)), we provide empirical evidence that co-trading networks are capable of capturing meaningful structures of the equity market. By visualizing a co-trading network, aggregated over the entire period of study, with information filtering (Rosario N Mantegna (1999)), we observe that stocks from the same sector groups tend to have strong co-trading relations. This observation echos the phenomenon that often stocks in the same sector groups of the market are likely to appear in the same portfolios and their prices tend to move together. Additionally, we uncover clusters, or communities, of stocks in the co-trading network. To detect these communities, we apply a spectral clustering algorithm on the co-trading matrix to group stocks with similar co-trading behaviors into clusters. For comparison, we select the Global Industry Classification Standard (GICS) as sector labels. Our empirical results show substantial overlap between the data-driven clusters and GICS sectors, which confirms that the co-trading network accommodate the sector structures as expected. Moreover, we leverage the uncovered network to study the influence of both individual stocks and sectors on the market. By using tools such as eigenvector centrality (Bonacich (1972), Bonacich (1987)), we identify that large technology companies and financial institutions, such as Microsoft, Apple, and JPMorgan, present strong co-trading relations with others, and thus have high impact on the structure of the market. Despite the alignment with GICS sectors, the co-trading network contains information beyond sectorial structure. The data-driven clusters also group together closely related stocks from different sectors.

Apart from the aforementioned static graph, the construction of co-trading matrices is flexible due to the choice of distance in time at which two trades are deemed to co-occur. It is also informative to analyze the time evaluation of co-trading networks and explore the dynamic of market structures. In this study, we focus on network time series at daily level, but this approach can easily be generalized to intraday, monthly and so forth. Our empirical findings from daily co-trading networks indicates that the co-trading relations across different sectors increase from 2017 to 2019. Using spectral clustering, we detect clusters at a daily level and compare them with GICS sectors. By A plot of the similarity across time reveals a downward trend with fluctuations. In addition, we also compare the similarity among daily clusters. The variation in clusters also increases as the spread of co-trading beyond sector groups. By applying a spectral clustering algorithm (Shi and Malik (2000); Ng, Jordan, and Weiss (2002); Cucuringu, Davies, et al. (2019); Cucuringu, Li, et al. (2020)) for change-point detection based on the temporal similarity heatmap, we uncover three distinct regimes over the period of study.

To exploit the association between co-trading behaviors and price co-movements, we conduct network regression analysis. We build realized covariance matrices from intraday returns as proxies for co-movements among stocks. By regressing covariance matrices against co-trading networks on a daily basis, we reveal positive associations between the two types of matrices. On 98.51% of the days in the study, the positive regression coefficients are statistically significant at 5% significance level. Further controlling for GICS sectors, we conduct multiple regressions by adding a fixed sector network as an independent variable. Even with the presence of sectors,

the positive and significant relation still holds. Furthermore, after removing price co-movements that arise from factor structures, the co-trading matrices capture patterns in the idiosyncratic covariance among stocks. Therefore, there is a strong indication that the co-trading behaviors at the high-frequency level are positively correlated with the return covariance, and have explanatory power on price co-movements that goes beyond the common risk factors and commonly adopted sectors.

With the aid of co-trading matrices, we propose a robust estimator for the high-dimensional covariance matrix of stock returns at daily frequency. By assuming that stock returns follow a linear factor structure (Ross (1976)), we decompose the covariance matrix as the sum of the factor covariance and the idiosyncratic covariance. Then, we impose a block structure on the diagonal of the idiosyncratic covariance matrix, such that elements outside the blocks are set to zero. Our approach extends the work of Ait-Sahalia and Xiu (2017), which uses principal component analysis to derive latent factors and form blocks using GICS sectors. However, as the GICS sectors are fixed, the sector blocks remain static over time. As we have shown, the market structures are time-varying, and thus static sector memberships do not suffice to capture the similarity of stocks at higher frequency. Therefore, we update the diagonal block structure daily with data-driven clusters derived from co-trading networks. To evaluate the performance, we construct mean-variance portfolios, subject to various leverage constraints. Our covariance estimators, based on dynamic clusters, generally outperform the baselines, using fixed GICS sectors, by achieving lower volatility and higher Sharpe ratios. Our best-performing portfolio achieves a Sharpe ratio of 1.40, which is 0.43 higher than the corresponding baseline of 0.97, thus giving a 44% improvement, and 0.57 higher than the market (0.83) over the same period.

The remainder of this paper is organized as follows. Section 2 outlines the contributions of this work to the existing literature. Section 3 introduces the definition of co-trading score and the construction of co-trading networks. In Section 4, we begin our empirical studies with conducting exploratory analysis on a static co-trading network and detecting clusters. Next, we study the dynamics of the daily co-trading matrices in Section 5. Subsequently, we explore the relation between daily co-trading networks and covariance matrices in Section 6 and propose a co-trading based covariance estimator in Section 7. Then, Section 8 provides a robustness analysis of the proposed estimator. Finally, in Section 9, we conclude and discuss limitations and potential research directions. The Appendices contain details of the spectral clustering algorithm and robustness analysis.

2 Literature review

This study sits at the confluence of three strands of literature. Firstly, our research enriches the network analysis and the modeling of complex inter-dependency relations in financial markets. Network analysis has been proven to be effective in studying inter-dependency relations in complex systems; in particular, there is a large literature on networks in financial markets (Bardoscia et al. (2021); Marti et al. (2021)).

Previous research develops various methodology to build financial networks. The influential work of Rosario N Mantegna (1999) first builds a network from a distance measure based on correlations of stock returns, which is then filtered with a minimum spanning tree (MST). Many works followed by constructing networks with diverse distance and similarity measures, such as return correlations (Tumminello, Di Matteo, et al. (2007); Di Matteo, Pozzi, and Aste (2010)), Granger causality (Billio et al. (2012)), mutual information (Fiedor (2014)), co-jumps of stock prices (Ding et al. (2021)), and so forth. Additionally, multiple methods have been used to replace MST for information filtering, including random matrix theory (Plerou et al. (2000)), Potts super-paramagnetic transitions (Kullmann, Kertesz, and R. Mantegna (2000)), planar maximally filtered graph (Tumminello, Aste, et al. (2005); Massara, Di Matteo, and Aste (2016)), a threshold-filter method (W.-Q. Huang, Zhuang, and Yao (2009); Namaki et al. (2011)), and

more. Recent works apply deep learning and natural language processing techniques to construct networks of various types of relations among stocks, such as company competition, product similarity, and news co-occurrence, from diverse data sources, such as financial reports, media news, and events (Hoberg and Phillips (2016); Schwenkler and Zheng (2019); Cheng et al. (2022); Yanci Zhang et al. (2023)).

Regarding networks of financial markets, preceding studies uncover the topological structures of markets through community detection. For example, the pioneering work of Rosario N Mantegna (1999) applies hierarchical clustering and discovers hierarchical structure stock portfolios. Moreover, the networks can be constructed as a time series (McDonald et al. (2005); Nie (2017)). Bennett, Cucuringu, and Reinert (2022) and Yichi Zhang et al. (2023) build lead-lag networks with different similarity measures, test multiple clustering algorithms and study time-varying lead-lag structures in the market.

To this field, our contribution is firstly, the proposal of an original similarity measure, directly derived from very granular records of trades, with explicit interpretation as how frequently two stocks are traded together, with the final goal of constructing networks. In addition, we detect dynamic clusters and provide a comprehensive comparison with GICS sectors.

Secondly, this research contributes to the studies of market microstructure, especially interplay among trading activities. Kyle (1985) posits a famous two-period model of high-frequency price formation by solving the equilibrium of the game between liquidity takers and market makers. Furthermore, various studies show that high-frequencies strategies can be aggressive. Hirschey (2021) claims that high-frequency traders (HFTs) can predict order flows from other market participants and trade ahead of them. Van Kervel and Menkveld (2019) provide empirical evidence that HFTs can detect the trading activities of institutional traders, and adjust their own trading strategies. Moreover, HFTs even actively explore the market by initiating small trades and watching the response of others (Clark-Joseph (2013)). Researchers also propose theoretical models for the interactions between HFTs and other traders (Grossman and Miller (1988); Brunnermeier and Pedersen (2005); Yang and Zhu (2020)).

The interactions can span across different stocks on the market. Bernhardt and Taub (2008) state that the strategical interplay among speculators is often concurrent and across many stocks. There is vast literature on cross-impact (Pasquariello and Vega (2015); Benzaquen et al. (2017); Schneider and Lillo (2019)), showing order flow of a stocks can affect prices of other stocks. Lu, Reinert, and Cucuringu (2022) classify trades of stocks by whether they concurrently arrive with other trades for the same or different, or both same and different stocks, and investigate price impact using order imbalance from different groups of trades. They discover that the time proximity of trade arrivals has explanatory power for stock returns.

This study uses the paper Lu, Reinert, and Cucuringu (2022) as starting point but instead considers interactions between the trades of every pair of stocks. Rather than studying the price impact of order imbalance on one stock at a time, we construct co-trading networks of all stocks jointly and study the impact of trading interactions at market microstructure level on macroscopic price co-movements.

Finally, our study adds to the growing body of financial econometrics literature on robust estimation of high-dimensional covariance matrices of stock returns. An invertible and well-behaved covariance matrix is essential for portfolio allocation with mean-variance optimization (Markowitz (1952)). However, when the number of sampled timestamps is small relative to the size of the panel of stocks, sample covariance matrices can be singular or ill-conditioned. To overcome this issue, previous studies develop different streams of regularized estimation methods, including thresholding (Bickel and Levina (2008b); Bickel and Levina (2008a)), shrinkage (Ledoit and Wolf (2003); Ledoit and Wolf (2004); Chen et al. (2010)), etc. These regularization techniques are based on structural assumptions; for example, thresholding estimators assume the covariance matrices are sparse. In particular for stocks, a large literature of asset pricing studies reveal linear factor structures of equity returns (Sharpe (1964); Ross (1976); Fama and

French (1992); Fama and French (1993); Fama and French (2015)). Based on factor models, the covariance matrix of returns can be decomposed as sum of a low-rank factor component and a residual idiosyncratic component. Various lines of work have then imposed different types of sparsity assumptions on the residual component which represents the covariance of idiosyncratic risk of stocks. Fan, Liao, and H. Liu (2016) provide a through overview of factor-based robust covariance estimation. By using observable and latent factors, respectively, the works of Fan, Furger, and Xiu (2016) and Ait-Sahalia and Xiu (2017) impose block structures on the idiosyncratic component, where stocks are sorted by their GICS sector membership, thus forcing the residual covariance of stocks in different sectors to be zero. Consequently, they conclude that incorporating clusters with economic interpretation benefits the covariance estimation task.

Our method for robust estimation contributes to this body of literature, and can be construed as a direct extension of the two aforementioned articles, by taking into account very granular high-frequency data that encodes higher-order relationships on the co-trading behavior. Instead of employing static GICS sectors, we perform time-varying data-driven clustering. By capturing the dynamic dependency relations between the universe of stocks, our proposed method outperforms baselines in portfolio allocation tasks.

3 Construction of co-trading networks

In this section, we propose pairwise co-trading scores to measure the similarity between two stocks, using the *co-occurrence of trades* methodology from Lu, Reinert, and Cucuringu (2022). Then we leverage these scores to build affinity matrices and construct co-trading networks.

3.1 Co-occurrence of trades

We start with introducing notations and then define co-occurrence of trades. Here, we denote each trade as a 4-tuple. Let $x_k = (\tau_k, s_k, d_k, q_k)$ denote the information of the k^{th} trade, where we capture the following trade characteristics

- τ_k is the time when the trade occurs;
- s_k indicates name of the stock for which the trade is executed;
- $d_k \in \{\text{buy}, \text{sell}\}$ indicates whether the trade is buyer- or seller-initiated;
- q_k is the volume of the trade.

Then, for every trade x_k , we define a δ -neighbourhood of trades which are close in time

$$\mathcal{N}_{x_k}^\delta = \{x_a | a \neq k \text{ and } \tau_a \in (\tau_k - \delta, \tau_k + \delta)\},$$

where δ is a predefined threshold corresponding to time.

Following the definition of trade co-occurrence from Lu, Reinert, and Cucuringu (2022), we say that trade x_k *co-occurs* with x_l at level δ , denoted by $x_k \overset{\delta}{\sim} x_l$, if and only if $x_l \in \mathcal{N}_{x_k}^\delta$. Figure 1 visualizes the definition, where x_k co-occurs with x_l and x_m , but does not co-occur with x_n . Trade x_n co-occurs with x_m , and both trade x_l and trade x_m co-occur with trade x_k , but they do not co-occur with each other.

The co-occurrence relation is symmetric, that is, given δ , if $x_k \overset{\delta}{\sim} x_l$, then $x_l \overset{\delta}{\sim} x_k$. Notice that co-occurrence of trades is not an equivalence relation. When it is clear from the context, we omit the level δ of the co-occurrence when referring to co-occurrence.

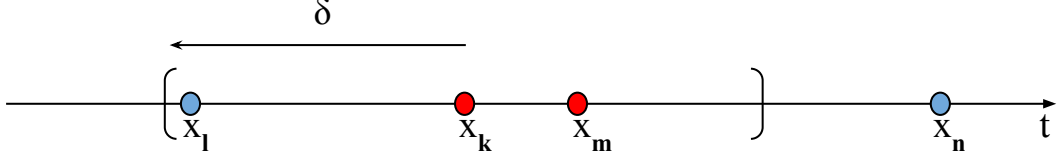


Figure 1: Illustration of trade co-occurrence. This figure visualizes the idea of co-occurrence of trades. With a pre-defined neighbourhood size δ , trade x_l arrives within the δ -neighbourhood of trade x_k , and thus they co-occur. In contrast, trade x_n locates outside x_k 's δ -neighbourhood, and thus the two trades do not co-occur. Trade x_n co-occurs with x_m , and both trade x_l and trade x_m co-occur with trade x_k , but they do not co-occur with each other. Adapted from Figure 1 in Lu, Reinert, and Cucuringu (2022).

3.2 Pairwise co-trading score

Motivated by the intuition that stocks are more inter-dependent if they are co-traded together more often, we propose pairwise co-trading scores to measure the similarity between stocks. For a pair of stocks, we calculate the similarity score by counting selected types of co-occurred trades and normalize by the total number of trades of both stocks.

The formal definitions are as follows. We assume a finite universe of N stocks. For stock i on day t , the set of all trades, with direction $d^i \in \{buy, sell, all\}$, is denoted by

$$S_t^{i,d^i} = \{x_a | \tau_a \in [t_{open}, t_{close}], s_a = i, d_a = d^i\},$$

where $d^i = all$ denotes all trades without distinguishing between buy and sell, and t_{open} and t_{close} stand for the time of market open and close respectively on day t . Then, if given another set S_t^{j,d^j} , we count the number of trades for stock j , which co-occur with trades in S_t^{i,d^i} , denoted as

$$L_{t,j \rightarrow i}^{d^j \rightarrow d^i} = \sum_{x_k \in S_t^{i,d^i}} |\{x_a \in \mathcal{N}_{x_k}^\delta | s_a = j, d_a = d^j\}|,$$

where $|\cdot|$ denotes the cardinality of a set.

The pairwise co-occurrence count index $c_{t,i,j}^{\delta,d^i,d^j}$ is a scaled count of the number of trades for stock i with direction d^i , and trades for stock j with direction d^j , which co-occur on day t . Formally, it is defined as

$$c_{t,i,j}^{\delta,d^i,d^j} := \frac{L_{t,i \rightarrow j}^{d^i \rightarrow d^j} + L_{t,j \rightarrow i}^{d^j \rightarrow d^i}}{\sqrt{|S_t^{i,d^i}|} \sqrt{|S_t^{j,d^j}|}}.$$

These pairwise co-occurrence indices have three useful properties. First, they are non-negative and higher values indicates stronger co-occurrence relations. Second, the indices are scaled, so that they can be used to compare relations across pairs of stocks. Third, the indices are symmetric. Additionally, the indices are defined using sets of trades which are filtered based on different conditions so that they are flexible and can easily be generalized to a customized set of orders.

3.3 Co-trading matrices and networks

Using the pairwise co-occurrence measures, we build the corresponding daily $N \times N$ co-occurrence matrix, denoted as $\mathbf{C}_t^{\delta,d^i,d^j}$, having entries

$$(\mathbf{C}_t^{\delta,d^i,d^j})_{i,j} = c_{t,i,j}^{\delta,d^i,d^j}.$$

Built from daily matrices, co-occurrence matrices over a longer time period T , such as months and years, are simply calculated by averaging the daily co-occurrence matrices;

$$\mathbf{C}_{\{T\}}^{\delta, d_i, d_j} = \frac{1}{|T|} \sum_{t \in T} C_t^{\delta, d_i, d_j}.$$

Taking advantage of the symmetric co-occurrence matrices, we build co-occurrence networks to represent complex structures in the stock market. We consider dynamic co-trading networks of stocks, $G_t = (V_t, E_t)$, $t \in T$, where each vertex $v_{i,t} \in V_t$ represents a certain stock at time t and a weighted edge $e_{i,j}(t) \in E_t$ denotes a type of co-occurrence relation between two stocks at time t ; the weight is the corresponding co-trading score. We use the co-trading matrices as representations of each co-trading network. The empirical study in the following sections focuses on the co-trading matrices without taking into account the directions of trades. In line with Lu, Reinert, and Cucuringu (2022), we choose $\delta = 500$ microseconds as the neighborhood size, in order to determine co-occurring trades. Therefore, we omit the superscripts for brevity and only keep the subscript for time index, e.g. $\mathbf{C}_{2017-2019}$ stands for the co-trading network aggregated from 2017 to 2019.

4 Empirical network analysis

In this section, we construct a co-trading network of the whole period of study from the empirical data. We provide a visualization of the network, and show that the co-trading matrix reflects empirical phenomena which have been observed in equity markets. Furthermore, we demonstrate that a co-trading network can capture inter-dependency of stocks beyond GICS sectors.

4.1 Data

The empirical studies in this paper are based on 457 stocks in US equity markets from 2017-01-03 to 2019-12-09. The 457 stocks are those constituents of the Standard & Poor’s (*S&P*) 500 index which have order book and price data available over the entire period of study.

We acquire limit order book data from the LOBSTER database (R. Huang and Polak (2011)), which keeps track of submissions, cancellations and executions of limit orders for stocks traded in NASDAQ. Each record has a timestamp with precision up to 10^{-9} seconds and indicates the price, size and direction of the respective order book event. A trade occurs when a market/marketable order arrives and consumes existing limit orders, and thus can be inferred by order executions. Here we denote a trade as ‘buyer-initiated’ if the limit order denoted a willingness to sell, and as ‘seller-initiated’ if the limit order denoted a willingness to buy. To derive trades, we filter out events other than executions. Then we aggregate records with exactly the same timestamp and direction, as they are likely to be caused by one large marketable order. The direction of a trade is opposite to those of the executed limit orders it is matched against.

In addition, we obtain minutely price data from LOBSTER and daily stock prices from the Center for Research in Security Prices (CRSP) database. Apart from prices, we label stock sectors using the Global Industry Classification Standard (GICS) drawn from the Compustat database. The GICS decomposition classifies stocks into 11 sectors of varying sizes.

4.2 A co-trading network

To provide a general view of co-trading, we construct a network-based matrix $\mathbf{C}_{2017-2019}$, capturing all co-trading relations of the entire period of study from 2017-01-03 to 2019-12-09, without differentiating directions of trades.

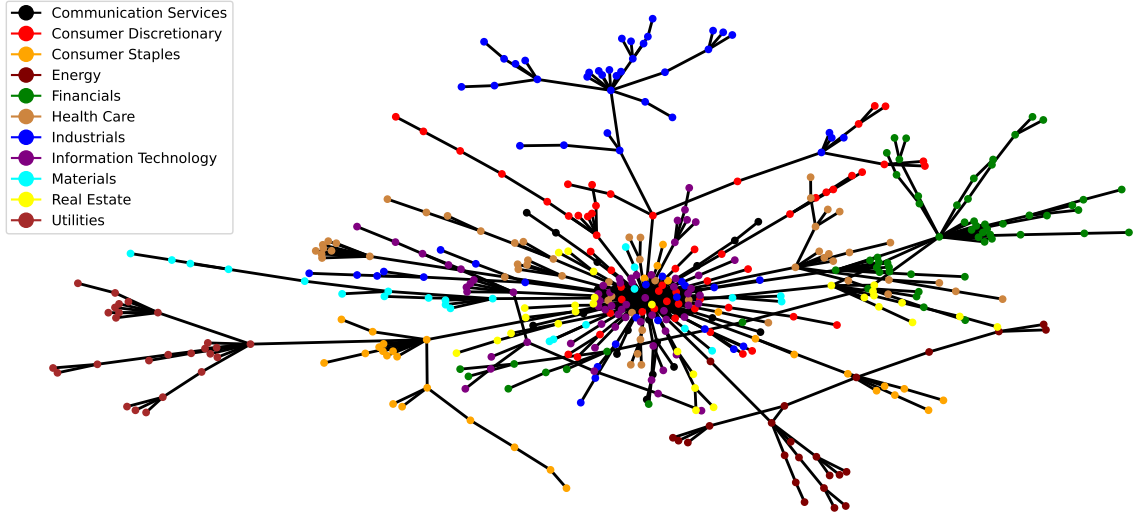


Figure 2: A co-trading network of the period from 2017-01-03 to 2019-12-09.

The figure presents the co-trading network of 457 stocks represented by the co-trading matrix, without trading directions, of the entire period of study, that is $\mathbf{C}_{2017-2019}$. Each node represents a stock, whose color indicates its GICS sector. For visualization, we use a maximum spanning tree (Rosario N Mantegna (1999)) to filter out edges by maximizing sum of co-trading scores while keeping a connected network with 456 edges.

To visualize the network, we follow Rosario N Mantegna (1999) and filter edges using a minimum spanning tree (MST), because the co-trading matrix is dense. To be specific, a MST of a graph with N nodes is a connected subgraph with only $N - 1$ edges such that the sum of the negations of edge weights is minimized, which can be found by Kruskal’s algorithm (Kruskal (1956)). For the implementation, we use the Python package ‘NetworkX’ (Hagberg, Swart, and S Chult (2008)) to filter edges and visualize networks. Figure 2 shows the MST of the co-trading network based on all trades of all stocks. The graph vertices represent individual stocks and their colors indicate the GICS sectors. It is noteworthy that companies within the same sector groups are often on the same branches, suggesting that stocks may frequently be co-traded in sector baskets. This chimes with the known fact that stocks in the same sector tend to move together, due to common membership in the same index traded funds (Harford and Kaul (2005)) and similar exposure to the same factors. Hence, this co-trading network captures meaningful patterns of the cross-sectional structure of stocks.

Furthermore, the network visualization reveals a dense cluster at the center of the plot. The stocks close to the centroid co-trade with more stocks and are, on average, more inter-related with the rest of the network, compared to the stocks at the leaves of the network. To further investigate the cluster, we use eigenvector centrality (Bonacich (1972), Bonacich (1987)) to measure the influence of each node on the network. For each stock i , the eigenvector centrality is the i th element of the eigenvector corresponding to the dominant eigenvalue of the co-trading matrix. The larger the centrality, the more “influential” the stock.

We list the 10 stocks with the highest eigenvector centrality in Table 1. Microsoft is the most influential stock, followed by Apple and JPMorgan Chase. Moreover, among the top 10 stocks, 60% are technology companies, including Facebook, and 40% are financial institutions. Moreover, the co-trading matrix does not only model individual stocks, but it can also model relations among sectors. Following Bennett, Cucuringu, and Reinert (2022), we build a meta-flow network of sectors as follows. We group stocks by their sector labels, use the sectors as nodes in the meta-flow network, and use the average co-trading scores of stocks in each pair of sectors to be the sector co-trading scores, serving as edge weights in the meta-flow

network. Figure 3 pictures the fully connected sector network, where the edge width indicates the strength of co-trading. The strongest co-trading relation is between Information Technology and Communication Services. By comparing edge widths, we can identify which sectors are more closely co-traded with a given sector. For example, the Real Estate sector has a strong co-trading relation with the Financials sector, while it does not show a strong relationship with the other sectors. Moreover, we document centrality of each sector in Table 2, and find that Information Technology, Financials and Communication Services are the most influential sectors, while Real Estate and Utilities have the lowest eigenvalue centrality.

Table 1: Top 10 stocks by eigenvector centrality.

This table lists 10 stocks ranked by their eigenvector centrality, as well as their company names and GICS sectors.

Ticker	Centrality	Company	Sector
MSFT	0.12	Microsoft Corp.	Information Technology
AAPL	0.11	Apple Inc.	Information Technology
JPM	0.10	JPMorgan Chase & Co.	Financials
BRK.B	0.10	Berkshire Hathaway	Financials
TXN	0.10	Texas Instruments	Information Technology
FB	0.09	Facebook Inc.	Communication Services
V	0.09	Visa Inc.	Information Technology
AXP	0.09	American Express Co	Financials
PYPL	0.09	PayPal	Information Technology
C	0.08	Citigroup Inc.	Financials

Table 2: Centrality of sectors in the meta-flow network.

This table shows the eigenvector centrality of each GICS sector in the meta-flow network. The ‘Rank’ column reports the rank, in descending order, of each sector in terms of their centrality.

	Centrality	Rank
Information Technology	0.38	1
Financials	0.35	2
Communication Services	0.34	3
Industrials	0.33	4
Health Care	0.33	5
Consumer Staples	0.32	6
Consumer Discretionary	0.29	7
Energy	0.26	8
Materials	0.26	9
Utilities	0.21	10
Real Estate	0.20	11

4.3 Clustering analysis

So far, we have observed the presence of clusters, or communities, in the co-trading network of stocks. In the following part, we introduce an unsupervised clustering method to classify every stock, with the aim to group similar stocks into the same cluster. By conducting clustering analysis on the network of $\mathbf{C}_{2017-2019}$ in Figure 2, we show that the co-trading matrix not only captures sector structure, but also incorporates associations beyond sectors.

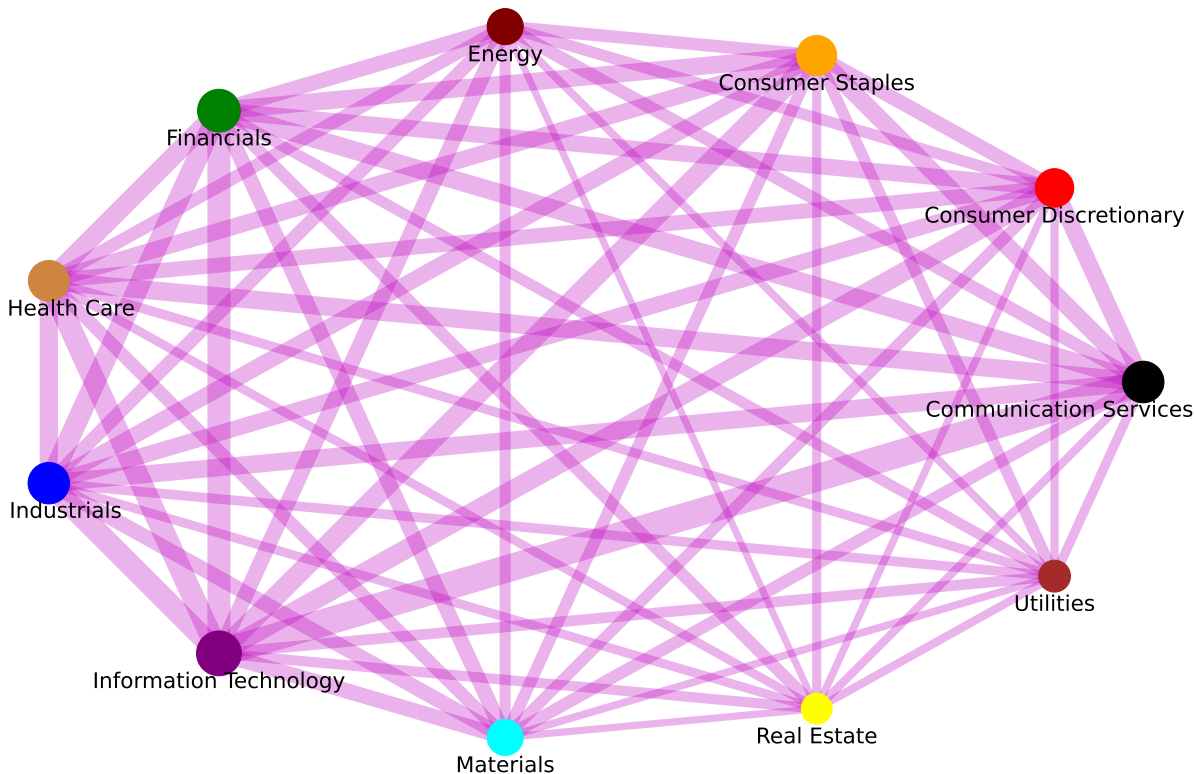


Figure 3: Meta-flow network of GICS sectors.

This figure illustrates the fully connected network of GICS sectors based on the co-trading matrix $C_{2017-2019}$. The edges are calculated by grouping stocks by their GICS sectors and averaging the co-trading scores of sector groups.

4.3.1 Methodology and evaluation metrics

Spectral clustering is a family of algorithms (Shi and Malik (2000); Ng, Jordan, and Weiss (2002); Cucuringu, Davies, et al. (2019); Cucuringu, Li, et al. (2020)), built upon spectral graph theory, to detect communities or clusters in networks. For details, Von Luxburg (2007) provides a comprehensive survey on spectral methods and their theoretical backgrounds. Given a co-trading matrix, we apply a spectral clustering algorithm, outlined in Appendix A, to identify clusters in our universe of stocks. The number of clusters is a hyper-parameter of this algorithm, which we need to determine beforehand. Although the spectral clustering depends on a random initialization, in Appendix B, we show that the algorithm is robust in our empirical setting.

The Adjusted Rand index (ARI) (Hubert and Arabie (1985)) is our measure of similarity between clusters. The valid range of ARI is $[-1, 1]$, where 1 is achieved if and only if two clusters perfectly match. Notice that ARI can take negative values, which means the two clusters are not similar at all. In general, a higher ARI indicates that two clusters are more similar to each other, and vice versa. A value close to 0 indicates that points are assigned into clusters almost randomly.

4.3.2 Data-drive clusters v.s. GICS sectors

We apply the spectral clustering method on the co-trading network. By analyzing the clusters, we discover that co-trading networks capture sectors in the US stock market, with an ARI of 0.56, which supports our observations in Section 4.2.

Figure 4 shows the commonality between GICS sectors and clusters detected in the co-occurrence network corresponding to the matrix $C_{2017-2019}$. By setting the number of clusters to 11, which is also the number of GICS sectors after the classification change in 2018, we observe

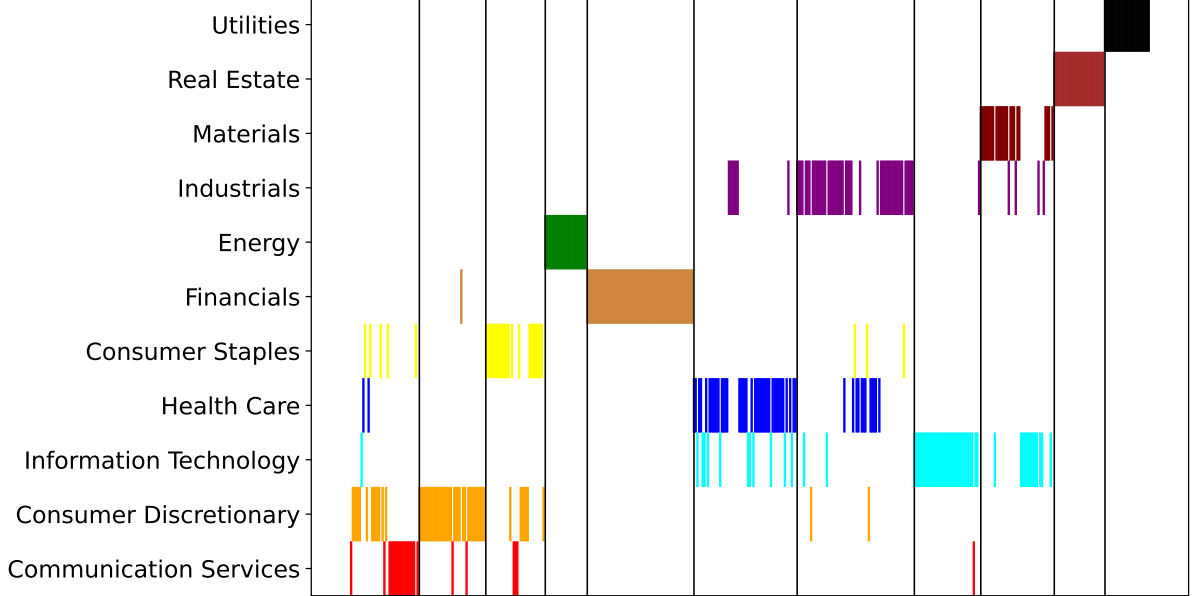


Figure 4: Clusters v.s. sectors.

This plot visualizes the overlap between the data-driven clusters, derived from $\mathbf{C}_{2017-2019}$ by spectral clustering, and the GICS sectors. The horizontal axis indexes stocks grouped by data-driven clusters, separated by vertical lines. The vertical axis indicates GICS sector labels. The colored area of a sector is indicative of its size.

that the unsupervised clustering method can recover the sector groups to a good standard. This is especially the case for companies in the Financial, Utilities, Real Estate and Energy sectors, when there are hardly any mismatches. There are also clear clusters for stocks in the sectors Materials, Health Care, Industrials and Consumer Staples, with small amounts of disagreements. Comparatively, the structure of the Information Technology sector is strikingly different, with one major cluster containing most of the stocks and most of the other stocks well spread out across other clusters. Moreover, the majority of stocks from the Consumer Discretionary sector concentrate in one cluster, and others are grouped with stocks in the Consumer Staples and Communication Services sectors.

5 Dynamics of co-trading networks and clusters

In addition to describing the long-term structure of the US equity market, time series of co-trading matrices built at higher frequencies contain information on the dynamic of topological structures of the market. We observe that co-trading across GICS sectors grows over time. To further explore, we compare the daily ARIs between generated clusters and GICS sectors and find a downward trend in their similarity. Moreover, we investigate the temporal changes of daily clusters and detect regime switching over the period of study.

5.1 Temporal evolution of co-trading networks

In Figure 5, we plot co-trading networks and their corresponding adjacency matrices, for the month of January, for the years 2017, 2018 and 2019, with colors representing the GICS sectors. After thresholding (W.-Q. Huang, Zhuang, and Yao (2009)), we only retain 1% of the edges, selected such that we preserve the edges with the highest weight. We find that the co-trading structures in the US equity market gradually change over the sample period. At the start of the period, the within-sector interactions are prominent, with only a few strong co-trading relations

across the GICS sectors. However, towards the end of the period, an increasing number of edges connect stocks from different sectors. The series of heatmaps clearly shows a pattern of decreasing within-sector co-trading connections, such as Financials, Real Estate, and Energy. In contrast, the strong co-trading connections of constituents of the Information Technology sector grow both within and across sectors. Co-trading relations among stocks in the Utility sector remain strong and isolated from other sectors over time. Therefore, the sets of stocks that speculators and investors tend to trade together in their portfolios are actually time-varying and deviate gradually from the standard GICS sectors. These findings also provide supporting evidence for the importance of dynamic data-driven clustering, that goes beyond the usual sector-based decomposition.

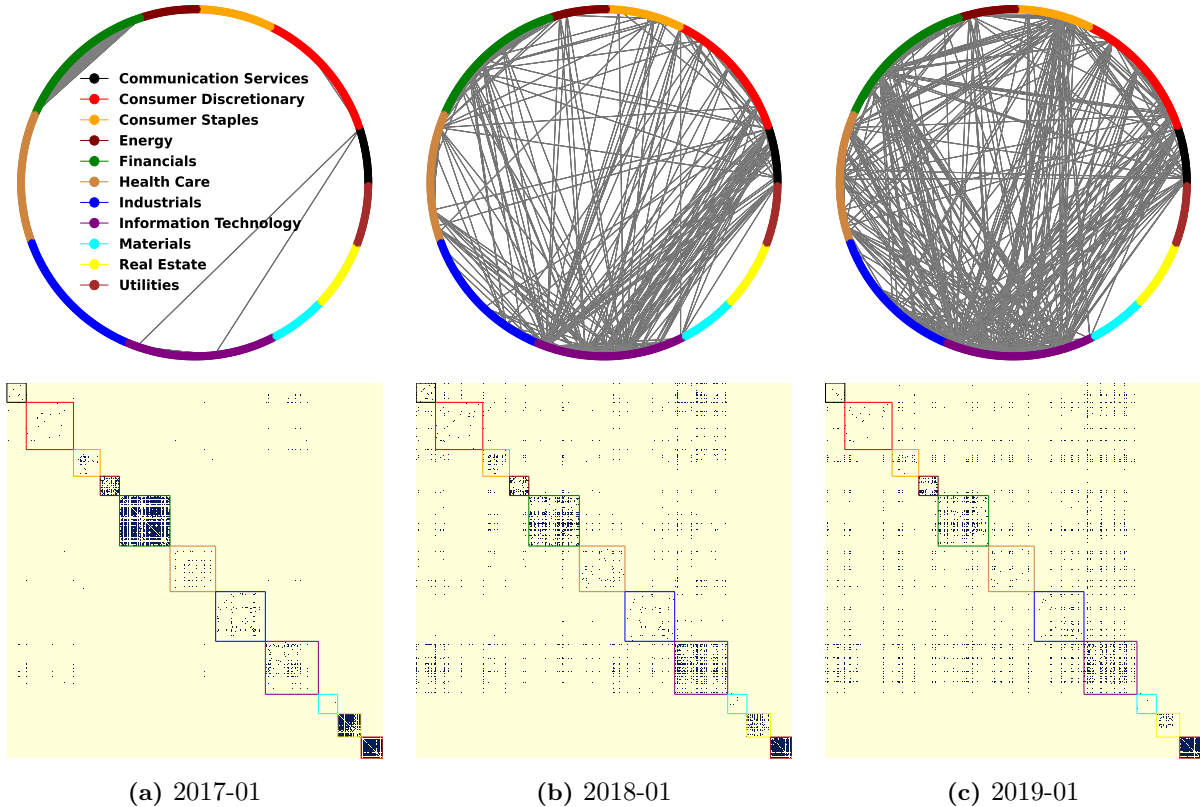


Figure 5: Thresholded temporal co-trading networks.

These three networks are based on co-occurrence of all trades regardless of trading directions. For visualization, we threshold on co-trading scores and only keep top 1% of edges. The first row contains the thresholded networks and the second row includes heatmaps of the corresponding co-trading matrices. From left to right, are networks and co-trading matrices of 2017-01, 2018-01 and 2019-01. Colors stand for the GICS sectors.

5.2 Temporal clustering analysis

Similar to uncovering long-term agreement between data-driven clusters and GICS sectors in Section 4.3, we are also interested in assessing and quantifying the extent to which the cross-sectional trading behaviors deviate from sectors within a short period of time. Therefore, we also proceed with clustering stocks on a daily basis, and then compare the similarity between clusters and sectors, via the same ARI measure. Since the true number of communities in the stock market is unknown, we consider multiple values for the number of clusters, namely 11 (the same number as the number of GICS sectors), 15, 20 and 50.

Figure 6 shows the time series of ARIs between daily clusters and GICS sectors. For a

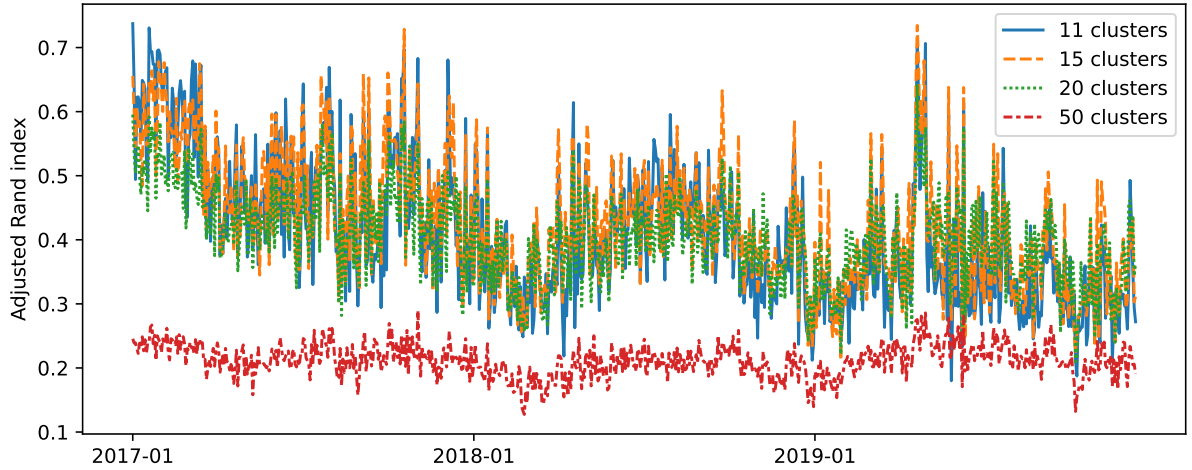


Figure 6: ARI between daily clusters and GICS sectors.

This figure sketches dynamics similarity between data-driven clusters and GICS sectors. For every day, we derive data-driven clusters and calculate the adjusted Rand index with GICS, with predefined numbers of clusters $\{11, 15, 20, 50\}$. We then plot the ARIs over time from 2017-01-03 to 2019-12-09, so that each line represents one choice of number of clusters.

Table 3: Statistics of daily ARI.

This table shows summary statistics of daily ARIs between dynamic clusters and fixed GICS sectors plotted in Figure 6. For different number of clusters, the table reports the mean and standard deviation of ARIs from 2017-01-03 to 2019-12-09, as well as the signal-to-noise ratio.

	Clusters			
	11	15	20	50
Mean	0.41	0.43	0.40	0.21
Standard deviation	0.11	0.10	0.07	0.03
Signal-to-noise ratio	3.73	4.30	5.71	7.00

small number of clusters, we observe meaningful levels of similarity between the data-driven clusters and economic sectors. In contrast, when the number is large as 50, the similarities are constantly low. As empirical observations indicate that market participants tend to trade sectors, we conclude that the true number of clusters is relatively small. Moreover, in Table 3 we summarize the mean and standard deviation of daily ARIs, for each choice of cluster numbers, over the entire period, echoing our visual findings. In addition, although the average ARI values of 11, 15 and 50 clusters are comparable, the variation drops by 0.03 as the number of clusters increases from 15 to 20, which is more conspicuous than the increase from 11 to 15. Based on the signal-to-noise ratio and taking the ARI into account, we settle to further investigate the case of 20 clusters.

Focusing on the temporal ARI curve of 20 clusters, we highlight two empirical findings. Firstly, at the daily frequency, co-trading behaviors align well with economic sectors, with frequent fluctuations. Secondly, we observe a downward trend in similarities, hinting that the sector structures become less prominent from 2017 to 2019. This reinforces the observation from Figure 5 concerning the growth of strong co-trading relations across GICS sectors. As expected, our co-trading networks embed dynamic structures in stock markets beyond static economic sectors.

5.3 Temporal stability of clusters and regime detection

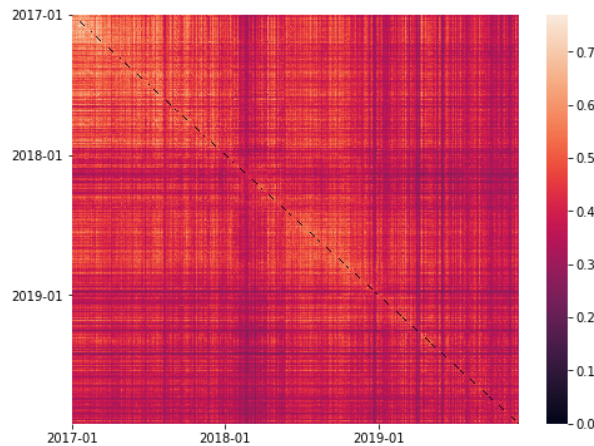


Figure 7: Similarity of daily clusters.

This heatmap shows the similarity between days. For every day, we group stocks into 20 clusters by applying spectral clustering on the daily co-trading matrix. Then, for each pair of days, we calculate the ARI between the clusters.

In addition to comparing daily clusters with the benchmark, we also measure the similarity between clusters corresponding to every pair of days. Figure 7 shows a heatmap of all such pairwise ARIs, based on 20 clusters. It is noteworthy that the colors along the diagonal get darker from upper left to lower right corner, which indicates that the market structures become unstable over time. Moreover, we distinguish three blocks along the main diagonal. For a quantitative regime detection, we apply the spectral clustering method (Appendix A) on the heatmap, and clearly identify three clusters of trading days, shown in Figure 8.

6 Co-trading and covariance

In this section, we connect the co-trading behavior to co-movement in stock prices. A direct measure of price co-movement is the covariance matrix. On every day t , we define a *realized*

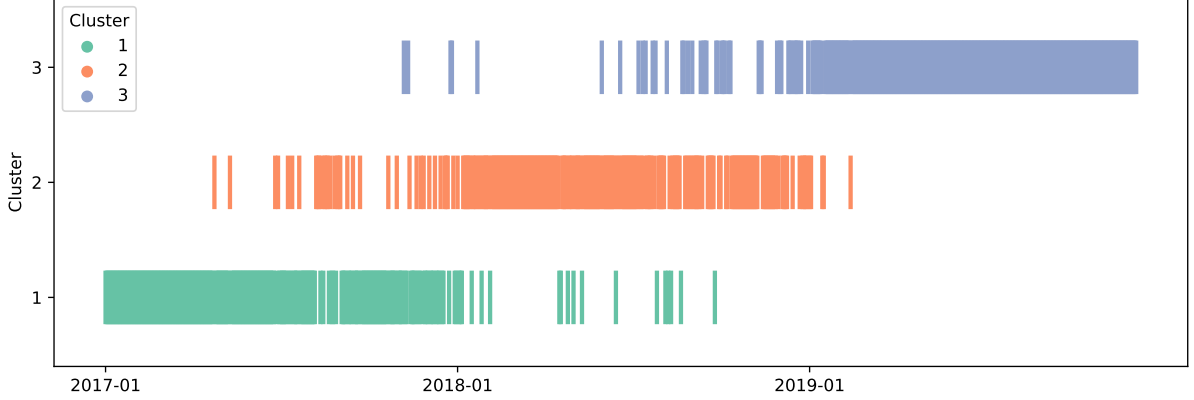


Figure 8: Regimes detected by spectral clustering.

This figure shows the clusters of days, derived by applying spectral clustering on the heatmap of ARI in Figure 7 to classify days into three regimes. The horizontal axis indicates dates and the vertical axis indicates which cluster each day belongs to.

covariance matrix, denoted as $\hat{\Sigma}_t^R$, as a proxy of the true covariance Σ_t , based on logarithmic returns of stocks. We conduct a regression analysis and uncover significant and positive associations between co-trading and realized covariance matrices. Furthermore, we find that co-trading matrices significantly explain the idiosyncratic covariance among stocks.

6.1 The realized covariance matrix and factor-based decomposition

For each day t , we define the *realized covariance matrix* following the three steps below. Since we only use intraday data, the index t is omitted in this part to avoid ambiguity. Firstly, we split the normal trading period from 9:30 to 16:00 into m equally spaced and non-overlapping intervals of length Δ . We denote $Int = \{\tau_1, \tau_2, \dots, \tau_m\}$ as the set of left end-points of each interval. Secondly, we define the logarithmic return of all stocks, $\mathbf{r}_\tau \in \mathbb{R}^N$, for each period, indexed by the left point of the interval τ , as

$$\mathbf{r}_\tau = \log(\mathbf{P}_\tau) - \log(\mathbf{P}_{\tau-\Delta}),$$

where $\mathbf{P}_\tau \in \mathbb{R}^N$ are mid prices at time τ . Finally, we build the realized covariance matrix as

$$\hat{\Sigma}^R = \sum_{\tau \in Int} \mathbf{r}_\tau \mathbf{r}_\tau^T.$$

For the empirical study in the following sections, we construct daily realized covariance matrices with sampling frequency of $\Delta = 5$ min, in line with Andersen et al. (2001); L. Y. Liu, Patton, and Sheppard (2015).

Furthermore, assuming that the intraday logarithmic stock returns, $\mathbf{r}_\tau \in \mathbb{R}^N$, at time τ , follow a linear K -factor model, they can be decomposed as

$$\mathbf{r}_\tau = \beta \mathbf{f}_\tau + \mathbf{u}_\tau,$$

where $\mathbf{f}_\tau \in \mathbb{R}^K$ is a vector of latent factors, $\beta \in \mathbb{R}^{N \times K}$ is a static loading matrix, and $\mathbf{u}_\tau \in \mathbb{R}^N$ is the idiosyncratic component which is assumed to be independent of \mathbf{f}_τ . Therefore, the covariance matrix of \mathbf{r}_τ can be decomposed as

$$\Sigma = \beta \Sigma^f \beta^T + \Sigma^u, \quad (1)$$

where $\Sigma^f = \sum_{\tau \in Int} \mathbf{f}_\tau \mathbf{f}_\tau^T$ is the low-rank covariance matrix of factors evaluated on the left

endpoints of the intervals, and $\Sigma^u = \sum_{\tau \in Int} \mathbf{u}_\tau \mathbf{u}_\tau^T$ is the idiosyncratic covariance. Ait-Sahalia and Xiu (2017) prove that, under additional assumptions, one can use the eigenvalues and eigenvectors to approximate the factor and idiosyncratic covariance matrices, and that the approximation errors are bounded. That is, one may write

$$\begin{aligned} \beta \Sigma^f \beta^T &\approx \sum_{k=1}^K \lambda_k \mathbf{v}_k \mathbf{v}_k^T, \\ \Sigma^u &\approx \sum_{k=K+1}^N \lambda_k \mathbf{v}_k \mathbf{v}_k^T, \end{aligned}$$

where λ_k is the k -th largest eigenvalue of Σ and \mathbf{v}_i denotes its corresponding eigenvector. Thus, we can write the sample covariance matrix as

$$\hat{\Sigma}^R = \sum_{k=1}^K \hat{\lambda}_k \hat{\mathbf{v}}_k \hat{\mathbf{v}}_k^T + \hat{\Sigma}^u, \quad (2)$$

where $\hat{\lambda}_k$ and $\hat{\mathbf{v}}_k$ are the k -th largest eigenvalue and eigenvector of the sample covariance matrix, and $\hat{\Sigma}^u = \sum_{k=K+1}^N \hat{\lambda}_k \hat{\mathbf{v}}_k \hat{\mathbf{v}}_k^T$ is the approximation of the idiosyncratic covariance. In the following empirical studies, we adopt four values of the number of latent factors, $K \in \{1, 3, 5, 10\}$.

6.2 Network regression analysis

In order to assess significance of the relationships between co-trading and covariance matrices, we perform a network regression on each day t

$$\hat{\Sigma}_t^R = \alpha_t \mathbf{1} + \gamma_t \mathbf{C}_t + \mathbf{E}_t, \quad (3)$$

where $\alpha_t \in \mathbb{R}$ is the intercept term, $\mathbf{1} \in \mathbb{R}^{N \times N}$ is an all-ones matrix, $\gamma_t \in \mathbb{R}$ is the regression coefficient, and $\mathbf{E}_t \in \mathbb{R}^{N \times N}$ is the residual matrix. As there are cross-sectional autocorrelations among stocks, it is not appropriate to assume independence in the residuals. Instead, to draw inference on the regression coefficients, we use the quadratic assignment procedure (QAP) (Mantel (1967), Krackhardt (1987), Krackhardt (1988)). This is a permutation test for comparing an observed matrix and an explanatory matrix; in the explanatory matrix, the order of the stocks is permuted, so that any correlation between the stocks in the two matrices is destroyed. We implement this and the other tests in this section using the R package ‘asnipe’ (Farine (2013)). Table 4 reports the regression coefficients. Positive relations between covariance and co-trading matrices appear in all days over the sample period, with mean and median of daily regression coefficients equal 5.10 and 4.48, respectively. Moreover, 98.51% of these positive relations are statistically significant at the 5% significance level.

In the next step, we assess whether co-trading networks explain cross-sectional variation in covariance beyond GICS sectors. To account for the sector structure in the regression, we introduce a static network of GICS sectors, as follows

$$\mathbf{S}_{i,j} = \begin{cases} 1, & \text{if stock } i \text{ and stock } j \text{ belong to the same cluster} \\ 0, & \text{otherwise.} \end{cases}$$

Then, controlling for the sector network, we perform the following regression

$$\hat{\Sigma}_t^R = \alpha_t \mathbf{1} + \gamma_t^C \mathbf{C}_t + \gamma_t^S \mathbf{S} + \mathbf{E}_t, \quad (4)$$

where $\alpha_t, \gamma_t^C, \gamma_t^S \in \mathbb{R}$ are the intercept and regression coefficients. We conduct a QAP in a

Table 4: Simple network regression.

This table reports the mean, median and standard deviation of daily network regression coefficients in (3), as well as their p -values. The p -values are obtained using the QAP with 2000 simulations. We run one regression for each trading day from 2017-01-03 to 2019-12-09.

	γ_t	p -value
Mean	5.10	0.005
Median	4.48	0.001
Standard deviation	2.86	0.034
Percentage positive	100	-
Percentage significant	98.51	-

multiple regression setting (MRQAP) (Krackhardt (1988)) using double semi-partialing (SDP) (Dekker, Krackhardt, and Snijders (2007)).

Table 5: Multiple network regression, realized covariance v.s. co-trading.

This table reports the mean, median and standard deviation of daily network regression coefficients in (4), as well as their p -values. We perform one regression for each trading day from 2017-01-03 to 2019-12-09. For inference, we use MRQAP with SDP, in line with Dekker, Krackhardt, and Snijders (2007) and simulate 2000 runs to calculate p -values.

	γ_t^C	p -value
Mean	3.61	0.030
Median	3.04	0.001
Standard deviation	2.52	0.116
Percentage positive	99.73	-
Percentage significant	89.81	-

The regression coefficients for the both co-trading and sector networks are shown in Table 5; they are highly significant, indicating that there is a relationship between the co-trading networks and the realized covariance matrix. It is noteworthy that the conclusion holds even when accounting for sectors. The mean and median of daily γ_t^C are 3.61 and 3.04, with 99.73% of positive values. During the whole sample period, 89.81% of the coefficients are statistically significant. As expected, sector networks are also positively correlated with price co-movements and significantly associated to the covariance structure of the stocks. With GICS sectors included in regressions, the coefficients of daily co-trading matrices are lower, since co-trading matrices evidently incorporate sector structures as well. Still, even then co-trading matrices have explanatory power on covariance of stocks beyond GICS sectors.

Furthermore, we find that the co-trading matrix captures some patterns in idiosyncratic covariance among stocks, beyond the common factors. We perform a factor-based covariance decomposition and regress idiosyncratic components against co-trading matrices with control for the sector network, as follows

$$\hat{\Sigma}_t^u = \alpha_t \mathbf{1} + \gamma_t^C \mathbf{C}_t + \gamma_t^S \mathbf{S} + \mathbf{E}_t, \quad (5)$$

where $\alpha_t, \gamma_t^C, \gamma_t^S \in \mathbb{R}$ are the intercept and regression coefficients.

We report the results in Table 6. For the K -factor model with $K = 1$, we remove the covariance on the direction of the first principal component from the realized covariance. Compared with Table 5, the average p -value decreases from 0.030 to 0.020, and the percentage of significant coefficients increases from 89.81% to 95.24%. Moreover, by separating the covariance of more latent factors, the coefficients become positive and significant over the whole period. Therefore,

the co-trading behaviors have explanatory power on the covariance of equity returns, beyond the price co-movements driven by common risk factors.

Table 6: Multiple network regression, idiosyncratic covariance v.s. co-trading.

This table reports the mean, median and standard deviation of daily network regression coefficients in (5), as well as their p -values. The ‘Factor’ column indicates the number of latent factors for covariance decomposition. We perform one regression for each trading day from 2017-01-03 to 2019-12-09. For inference, we use MRQAP with SDP, in line with Dekker, Krackhardt, and Snijders (2007) and simulate 2000 runs to calculate p -values.

Factor		γ_t^C	p -value
1	Mean	2.57	0.020
	Median	2.16	0.001
	Standard deviation	1.73	0.102
	Percentage positive	99.46	-
	Percentage significant	95.24	-
3	Mean	1.25	0.001
	Median	1.12	0.001
	Standard deviation	0.62	0.001
	Percentage positive	100.00	-
	Percentage significant	100.00	-
5	Mean	0.86	0.001
	Median	0.77	0.001
	Standard deviation	0.42	0.000
	Percentage positive	100.00	-
	Percentage significant	100.00	-
10	Mean	0.46	0.001
	Median	0.41	0.001
	Standard deviation	0.22	0.000
	Percentage positive	100.00	-
	Percentage significant	100.00	-

7 High-dimensional covariance estimation and application to portfolio allocation

The realized covariance matrices in Section 6 pertain to 457 stocks, but are constructed from 78 samples (corresponding to 5 minute buckets) for each stock. The parameter estimations thus fall into a high-dimensional setting where the number of samples is smaller than the dimension of the covariance matrix, resulting in singular estimates. However, it is important to have invertible and well-behaved estimates in practice, for tasks such as mean-variance portfolio allocation.

Fortunately, we have found significant associations between realized covariance, especially its idiosyncratic component, and co-trading matrices. With the aid of data-driven co-trading clusters, we develop a method for robust estimation of high-dimensional covariance matrices. This approach is motivated by the work of Ait-Sahalia and Xiu (2017), and can be construed as an extension of it that considers higher-order interactions by leveraging very granular high-frequency data that incorporates the dynamic topological structures of the network of stocks.

7.1 Robust covariance matrix estimation

With the proven capability of capturing dynamic communities in the market and patterns in idiosyncratic covariance, we propose a robust covariance estimator achieving positive definiteness by imposing a block structure on the idiosyncratic part of the sample covariance matrix, $\hat{\Sigma}^u$, based on the data-driven clusters derived from co-trading matrices. We first estimate the covariance matrix as in Section 6, and decompose each realized covariance matrix into factor and idiosyncratic components, as in (1). Next, we threshold the idiosyncratic covariance matrix to obtain a sparse matrix $\hat{\Gamma}^u$, whose element corresponding to the pair of stocks i and j is

$$\hat{\Gamma}_{i,j}^u = \begin{cases} \hat{\Sigma}_{i,j}^u, & \text{if stock } i \text{ and stock } j \text{ belong to the same cluster} \\ 0, & \text{otherwise.} \end{cases}$$

Our proposed covariance estimator, incorporating the co-trading clusters, is then given by

$$\hat{\Sigma}^{Cluster} = \sum_{k=1}^K \hat{\lambda}_k \hat{\mathbf{v}}_k \hat{\mathbf{v}}_k^T + \hat{\Gamma}^u.$$

The estimator is positive definite if the size of every cluster is smaller than the rank of the singular sample covariance matrix, which is usually the number of samples used to calculate it. To be specific, with a sampling frequency of 5 minutes, the largest cluster should contain no more than 78 stocks. In contrast to the paper Ait-Sahalia and Xiu (2017), which uses GICS sectors as a fixed ‘‘cluster’’, we can tune the number of clusters to guarantee positive definiteness given any universe of stocks. Moreover, thresholding with co-trading clusters embeds the dynamic of the dependency structure in stock markets, which is reasonable for covariance estimation at daily or higher frequency.

7.2 Mean-variance portfolio construction

To demonstrate economic value of the proposed robust covariance estimates, we develop a daily rebalanced mean-variance strategy, which opens positions at market open and liquidates at market close, for each trading day over the period of study. Based upon the assumption that $\mathbb{E}[\hat{\Sigma}_t | \hat{\Sigma}_{t-1}] = \hat{\Sigma}_{t-1} \in \mathbb{R}^{N \times N}$, we derive mean-variance portfolio weights $\mathbf{w}_t \in \mathbb{R}^N$, on day t , by solving the following constrained optimization

$$\begin{aligned} \min_{\mathbf{w}_t} \quad & \mathbf{w}_t^T \hat{\Sigma}_{t-1} \mathbf{w}_t \\ \text{s.t.} \quad & \mathbf{w}_t^T \vec{\mathbf{1}} = 1 \\ & \|\mathbf{w}_t\|_1 \leq l, \end{aligned} \tag{6}$$

where $\vec{\mathbf{1}}$ denotes the all-ones vector, and $l \geq 0$ restricts the level of leverage. When $l = 1$, leverage is not allowed and all weights are non-negative. In contrast, when $l = \infty$, short-sell is unrestricted and the optimization leads to the global minimum variance portfolio (GMV) (Jagannathan and Ma (2003); Bollerslev, Patton, and Quaedvlieg (2018)). In the special case that $l = \infty$, an analytical solution, $w_t = \frac{\hat{\Sigma}_{t-1}^{-1} \vec{\mathbf{1}}}{\vec{\mathbf{1}}^T \hat{\Sigma}_{t-1}^{-1} \vec{\mathbf{1}}}$, to the constrained optimization exists. Otherwise, we solve it numerically using the ‘CVXPY’ package in Python (Diamond and Boyd (2016); Agrawal et al. (2018)). Note that it is possible for $\hat{\Sigma}_{t-1}$ to be numerically singular. To avoid this issue, we do not trade on days with ill-behaved covariance estimates, and we set $\mathbf{w}_t = \vec{\mathbf{0}}$ if the condition number of $\hat{\Sigma}_{t-1}$ is greater than 1×10^9 . Finally, the daily portfolio return is calculated as

$$r_t^{mv} = \mathbf{w}_t^T \mathbf{r}_t,$$

where $\mathbf{r}_t \in \mathbb{R}^N$ is a vector of stock logarithmic open-to-close returns.

The evaluation metrics of portfolio performance are annualized volatility and Sharpe ratio.

The annualized volatility is calculated as

$$\sigma^{mv} = stdev(r_t^{mv}) \times \sqrt{252},$$

where $stdev(\cdot)$ is the standard deviation function. The annualized Sharpe ratio (Sharpe (1994)) is defined as

$$sr^{mv} = \frac{\overline{r^{mv}} \times 252}{\sigma^{mv}},$$

where $\overline{r^{mv}}$ denotes the average daily return of the portfolio. A high Sharpe ratio indicates lower portfolio volatility, adjusted by mean return.

7.3 Analysis of portfolio performance

In the following empirical portfolio analysis, we experiment with multiple values of the parameters corresponding to the number of data-driven clusters, number of factors for covariance estimation, and leverage constraints for optimization. For each set of parameters, we construct a daily portfolio, and perform a backtest over the period of study. Since we calculate portfolio weights traded on day t from covariance estimates from day $t - 1$, all of our tests are out-of-sample.

The annualized volatility of the portfolios is shown in Figure 9. We conclude that a larger number of clusters, which imposes higher level of sparsity on the residual covariance components, leads to more robust covariance estimation, and lower variation in portfolio returns. With short-sell prohibited, the portfolio risks are similar. As leverage constraints relax, the GICS portfolios with 11 fixed clusters and the portfolios corresponding to 15 co-trading clusters exhibit increasing annualized volatility. In contrast, when we consider 20 and 50 co-trading clusters, the annualized portfolio risks decrease, and stabilize at around 8%, regardless of the number of factors.

Figure 9 thus indicates that portfolios using our method of robust covariance estimation can lead to superior performance compared to portfolios built upon GICS sector-based covariance estimates. For further comparison after adjusting for returns, we add Sharpe ratios for selected portfolios in Table 7. In alignment with our findings from Figure 9, data-driven clusters outperform fixed GICS sectors for robust covariance matrix estimation. However, increasing the number of clusters too much deteriorates the Sharpe ratio. It is noteworthy that, with 50 clusters, the idiosyncratic covariance matrices are overly sparse and the covariance among stocks is underestimated. Thus the portfolio optimization tends to select stocks with lower volatility instead of diversifying, and results in low level of returns. From the numbers of clusters considered here, the highest Sharpe ratio of 1.40 is attained by the GMV for 20 clusters with 10 latent factors.

Zooming into the trajectory of portfolio gains, we sketch the cumulative returns of the best GMV portfolios for the data-driven clusters we propose, along with the GICS sector as a baseline, respectively, in Figure 10. Furthermore, we add the S&P 500 index (SPY ETF) as a proxy for the market. Clearly, trading SPY from open to close every day is not a profitable trading strategy. Apart from that, the portfolio derived from our method outperforms the GICS baseline and the market benchmark, by achieving comparable profits while bearing much smaller fluctuations and shorter drawdown periods.

8 Robustness analysis

In this section, we briefly discuss the robustness of the spectral clustering algorithm. Moreover, we report on the results when calculating co-trading scores based on traded volume instead of the number of trades. Further details of robustness checks are provided in the Appendix.

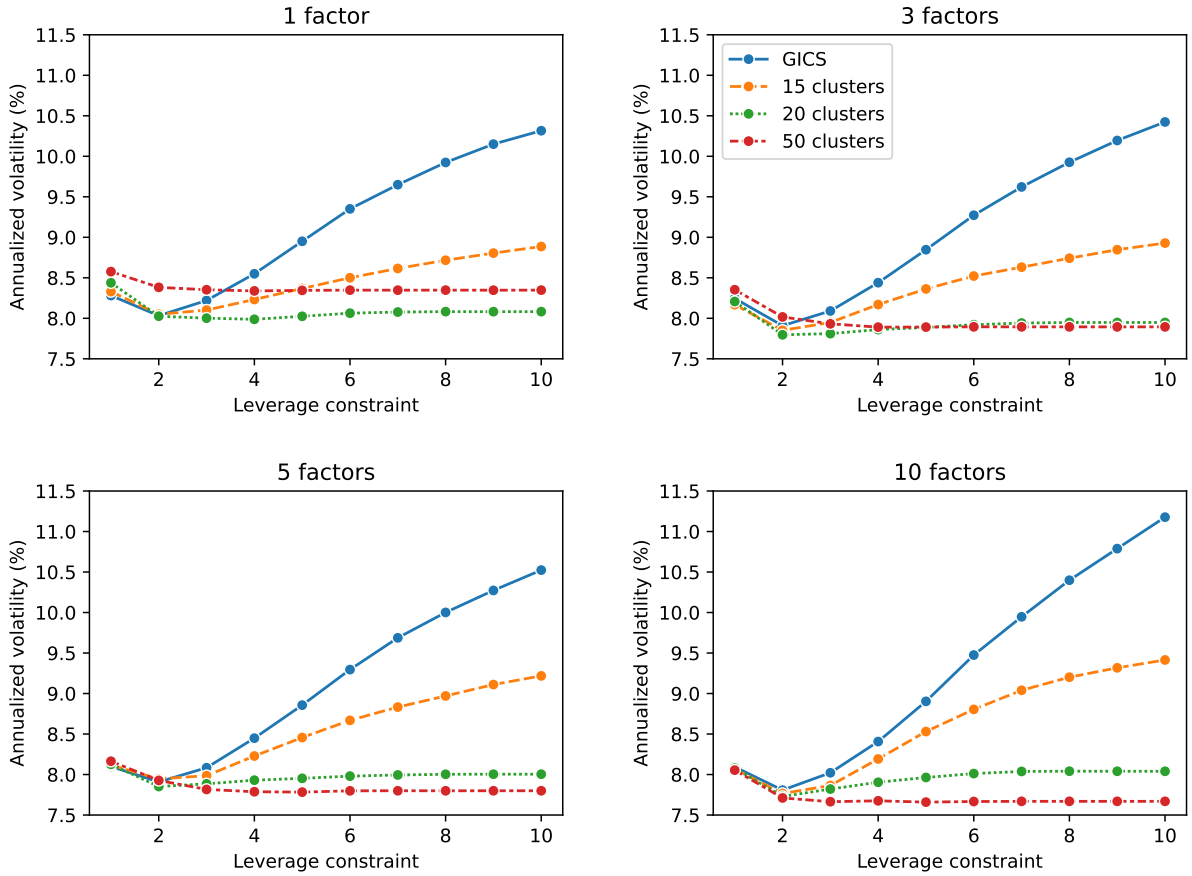


Figure 9: Annualized volatility of mean-variance portfolios.

These figures show the annualized volatility of mean-variance portfolios constructed by solving (6) based on different covariance matrices estimates. The out-of-sample backtests span the period from 2017-01-03 to 2019-12-09. Every sub-figure corresponds to one choice of latent factor numbers while decomposing sample covariance matrices in (1). In each sub-figure, every curve plots portfolio volatility, for a choice of blocks structure imposed on the residual covariance, along leverage constraints.

Table 7: Annualized Sharpe ratio of mean-variance portfolios.

This table documents the annualized Sharpe ratios of mean-variance portfolios constructed by solving (6) based on different covariance matrices estimates. The out-of-sample backtests span the period from 2017-01-03 to 2019-12-09. The ‘Factor’ column specifies the number of latent factors while decomposing the sample covariance matrices. The ‘Leverage’ column indicates leverage constraints in (6), where ∞ means that short-sell is unrestricted. We use 15, 20 and 50 clusters, together with GICS sectors as the baseline, while imposing diagonal block structure on the residual covariance matrices.

Factor	Leverage	Cluster			
		GICS	15	20	50
1	1	0.01	0.13	0.09	-0.06
	3	0.57	0.61	0.53	0.12
	5	0.75	0.89	0.69	0.12
	7	0.71	0.98	0.69	0.12
	∞	0.45	1.07	0.69	0.12
3	1	0.35	0.48	0.44	0.36
	3	0.54	0.74	0.86	0.51
	5	0.95	1.02	1.04	0.54
	7	0.92	1.13	1.11	0.54
	∞	0.59	1.19	1.12	0.54
5	1	0.38	0.52	0.51	0.47
	3	0.63	0.81	0.88	0.62
	5	1.04	1.11	1.16	0.70
	7	1.06	1.28	1.23	0.71
	∞	0.69	1.29	1.23	0.71
10	1	0.44	0.50	0.45	0.42
	3	0.64	0.89	1.04	0.58
	5	1.12	1.16	1.34	0.69
	7	1.27	1.28	1.39	0.70
	∞	0.97	1.18	1.40	0.70

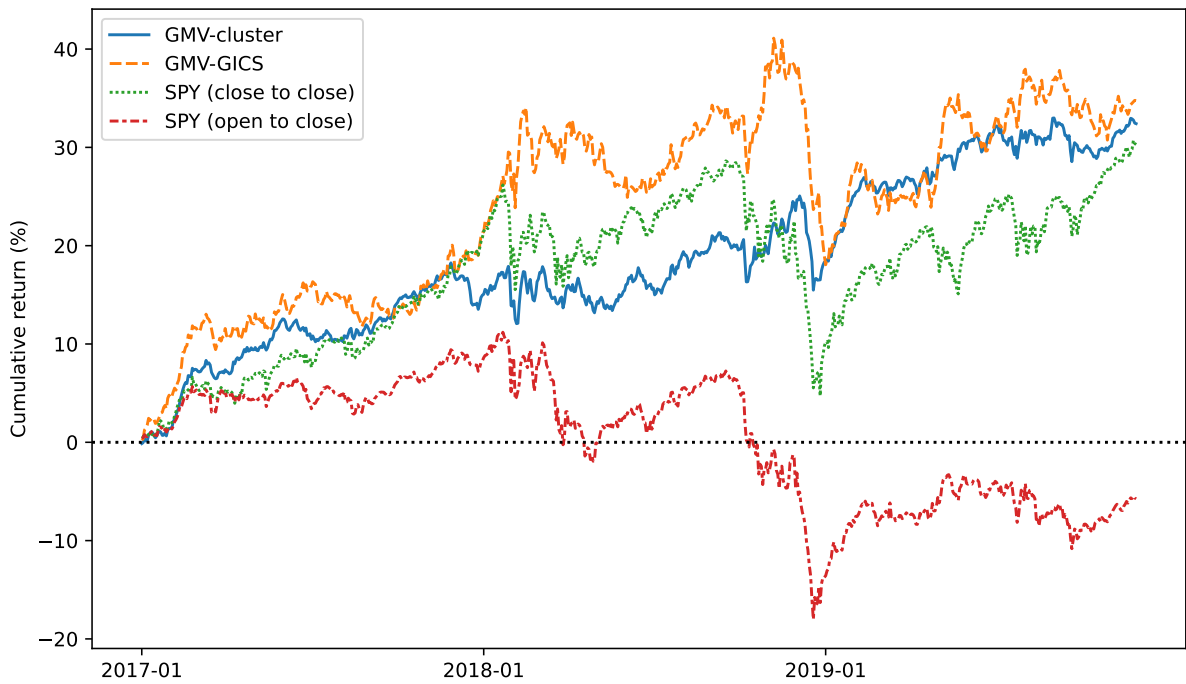


Figure 10: Cumulative returns of portfolios.

This figure plots cumulative returns of four portfolios from 2017-01-03 to 2019-12-09. The portfolios include (1) ‘GMV-cluster’: the global minimum variance portfolio based on robust covariance matrices estimated using our method with 10 factors and 20 clusters; (2) ‘GMV-GICS’: the GMV portfolio based on robust covariance matrices estimated using 10 factors and GICS sectors; (3) ‘SPY (close to close)’: the SPDR S&P 500 ETF Trust which tracks the S&P 500 Index; (4) ‘SPY (open to close)’: the SPY ETF, following our strategy, with positions only during normal trading hours.

8.1 Random initialization of spectral clustering algorithm

The spectral clustering algorithm applies K-means (MacQueen (1967)) on the spectral domain of the co-trading matrices. Thus, one first computes a low-dimensional embedding of the stocks given by the extremal eigenvectors of the graph Laplacian matrix associated to the co-trading network, and then performs clustering via K-means (Von Luxburg (2007)). An issue of K-means is that the clustering results may be sensitive to the random initialization. In order to mitigate this sensitivity, we adopt K-means++ (Arthur and Vassilvitskii (2006)) for the initialization. To further empirically examine the robustness, we repeat the experiment of clustering on daily co-trading networks in Section 5.2 in 100 trials, each time with a different random seed. Then we compare the daily means of ARIs between clusters from each pair of experiments. Our results ensure that the spectral clustering method we use is robust to finding clusters in co-trading networks. Further details are provided in Appendix B.

8.2 Volume-driven co-trading behavior

Instead of incorporating the number of transactions, we also explore the possibility of defining co-trading in terms of traded volumes. Details can be found in Appendix C. By comparing the ARIs between corresponding clusters and GICS sectors, we observe that volume based co-trading matrices share the same patterns as those measured in the number of transactions. According to the portfolio performance, described in Section 7, the Sharpe ratios of GMV portfolios corresponding to the volume-based co-trading matrices surpass the GICS benchmarks. Overall, our findings are robust under the volume measure, in the sense that they show similar patterns.

However, compared with the count of trades, using traded volume in measuring co-trading is less robust in terms of daily random seed tests and dynamic comparison with GICS sectors. Moreover, volume based co-trading matrices lead to inferior economic value compared to count-based matrices, when using the mean-variance portfolio analysis in Section 7. These findings echo previous research (Chan and Lakonishok (1995); Chordia and Subrahmanyam (2004)) which shows that, since institutions tend to split large orders to hide their liquidation purpose and reduce market impact, the number of transactions outperforms the volume in measuring price impact. We confirm that using count of trades better captures patterns in price co-movement.

9 Conclusion and future research directions

In this paper, we introduce and construct co-trading networks to model the dependency structure of stocks arising from the interaction of cross-stock trading among market participants, in response of trade arrivals on the market. Using a spectral clustering algorithm, we uncover clusters which capture well temporally evolving structures within markets, containing information beyond industry sectors. Our empirical studies, focusing on daily co-trading during 2017-01-03 to 2019-12-09, reveal that cross-stock trading behaviors are time-varying, and co-trading relations across different GICS sectors become apparent. These two observations indicate that solely relying on sectors is not sufficient for capturing co-trading behavior, and they motivate the construction and analysis of time series of co-trading networks built from very granular high-frequency data.

Taking one step further, we establish that strong co-trading relations can lead to a high level of co-movements in stock prices. We use realized covariance matrices to measure the co-movements of prices. Through network regression analysis, we document a significant positive relation between co-trading and covariance matrices, especially idiosyncratic covariance matrices. Even when adding a network of sectors as a control variable in the regression, the conclusion remains valid. This conclusion bridges the gap between cross-stock trading activities at the microstructure level and the macroscopic covariance of stock returns.

Employing dynamic co-trading networks and data-driven clusters, we develop a robust covariance estimator for stock covariance, in a situation where the number of samples for estimating the covariance is smaller than the number of stocks. Our method outputs well-behaved estimates from sample covariance matrices, by incorporating contemporaneous information of stock clusters. As a result, a mean-variance portfolio constructed with our robust estimates achieves lower volatility and higher Sharpe ratios in comparison with baseline methods and market returns.

Our concept of co-trading provides a general framework to investigate the interaction of trade flow corresponding to different stocks; for example, one could take into account the directions of trades, as defined in Section 3, when analyzing the co-trading behavior. It would also be worthwhile to further investigate how trades with same (resp., opposite) directions contribute to the positive (resp., negative) components of covariance and correlation of stocks. Additionally, in this study we assume that the co-trading score is symmetric; however, asymmetric scores may also be of interest, and the pairwise relationships could be modeled and clustered using methodology from the directed graph clustering literature (Cucuringu, Li, et al. (2020)). For convenience this paper assumes that the universe of stocks does not change across time; it could be interesting to include the possibility of some new stocks arriving and some existing stocks ceasing to trade. Intuitively, shocks on companies with large market cap can have impact on small cap stocks, but the converse is often not true. With a simple adjustment to the current co-trading scores, this asymmetry could be embedded into the network construction, allowing for the investigation of asymmetric spillover effects. Furthermore, it would be interesting to leverage the co-trading network time series for forecasting tasks concerning market structures, returns, and covariances, possibly combined with models ranging from parsimonious to deep learning.

References

- [1] Akshay Agrawal et al. “A rewriting system for convex optimization problems”. In: *Journal of Control and Decision* 5.1 (2018), pp. 42–60.
- [2] Yacine Ait-Sahalia and Dacheng Xiu. “Using principal component analysis to estimate a high dimensional factor model with high-frequency data”. In: *Journal of Econometrics* 201.2 (2017), pp. 384–399.
- [3] Torben G Andersen et al. “The distribution of realized stock return volatility”. In: *Journal of Financial Economics* 61.1 (2001), pp. 43–76.
- [4] David Arthur and Sergei Vassilvitskii. *k-means++: The advantages of careful seeding*. Tech. rep. Stanford, 2006.
- [5] Marco Bardoscia et al. “The physics of financial networks”. In: *Nature Reviews Physics* (2021), pp. 1–18.
- [6] Stefanos Bennett, Mihai Cucuringu, and Gesine Reinert. “Lead–lag detection and network clustering for multivariate time series with an application to the US equity market”. In: *Machine Learning* 111.12 (2022), pp. 4497–4538.
- [7] Michael Benzaquen et al. “Dissecting cross-impact on stock markets: An empirical analysis”. In: *Journal of Statistical Mechanics: Theory and Experiment* 2017.2 (2017), p. 023406.
- [8] Dan Bernhardt and Bart Taub. “Cross-asset speculation in stock markets”. In: *The Journal of Finance* 63.5 (2008), pp. 2385–2427.
- [9] Peter J Bickel and Elizaveta Levina. “Covariance regularization by thresholding”. In: *The Annals of Statistics* 36.6 (2008), pp. 2577–2604.
- [10] Peter J Bickel and Elizaveta Levina. “Regularized estimation of large covariance matrices”. In: *The Annals of Statistics* 36.1 (2008), pp. 199–227.

- [11] Monica Billio et al. “Econometric measures of connectedness and systemic risk in the finance and insurance sectors”. In: *Journal of Financial Economics* 104.3 (2012), pp. 535–559.
- [12] Tim Bollerslev, Andrew J Patton, and Rogier Quaadvlieg. “Modeling and forecasting (un) reliable realized covariances for more reliable financial decisions”. In: *Journal of Econometrics* 207.1 (2018), pp. 71–91.
- [13] Phillip Bonacich. “Factoring and weighting approaches to status scores and clique identification”. In: *Journal of Mathematical Sociology* 2.1 (1972), pp. 113–120.
- [14] Phillip Bonacich. “Power and centrality: A family of measures”. In: *American Journal of Sociology* 92.5 (1987), pp. 1170–1182.
- [15] Markus K Brunnermeier and Lasse Heje Pedersen. “Predatory trading”. In: *The Journal of Finance* 60.4 (2005), pp. 1825–1863.
- [16] Francesco Capponi and Rama Cont. “Multi-asset market impact and order flow commonality”. In: *Available at SSRN* (2020).
- [17] Louis KC Chan and Josef Lakonishok. “The behavior of stock prices around institutional trades”. In: *The Journal of Finance* 50.4 (1995), pp. 1147–1174.
- [18] Yilun Chen et al. “Shrinkage algorithms for MMSE covariance estimation”. In: *IEEE Transactions on Signal Processing* 58.10 (2010), pp. 5016–5029.
- [19] Dawei Cheng et al. “Financial time series forecasting with multi-modality graph neural network”. In: *Pattern Recognition* 121 (2022), p. 108218.
- [20] Tarun Chordia and Avanidhar Subrahmanyam. “Order imbalance and individual stock returns: Theory and evidence”. In: *Journal of Financial Economics* 72.3 (2004), pp. 485–518.
- [21] Adam Clark-Joseph. “Exploratory trading”. In: *Unpublished job market paper. Harvard University, Cambridge, MA* (2013).
- [22] Mihai Cucuringu, Peter Davies, et al. “SPONGE: A generalized eigenproblem for clustering signed networks”. In: *The 22nd International Conference on Artificial Intelligence and Statistics*. PMLR. 2019, pp. 1088–1098.
- [23] Mihai Cucuringu, Huan Li, et al. “Hermitian matrices for clustering directed graphs: insights and applications”. In: *International Conference on Artificial Intelligence and Statistics*. PMLR. 2020, pp. 983–992.
- [24] David Dekker, David Krackhardt, and Tom AB Snijders. “Sensitivity of MRQAP tests to collinearity and autocorrelation conditions”. In: *Psychometrika* 72.4 (2007), pp. 563–581.
- [25] Tiziana Di Matteo, Francesca Pozzi, and Tomaso Aste. “The use of dynamical networks to detect the hierarchical organization of financial market sectors”. In: *The European Physical Journal B* 73 (2010), pp. 3–11.
- [26] Steven Diamond and Stephen Boyd. “CVXPY: A Python-embedded modeling language for convex optimization”. In: *Journal of Machine Learning Research* 17.83 (2016), pp. 1–5.
- [27] Yi Ding et al. “Stock co-jump networks”. In: *Available at SSRN* (2021).
- [28] Eugene F Fama and Kenneth R French. “A five-factor asset pricing model”. In: *Journal of Financial Economics* 116.1 (2015), pp. 1–22.
- [29] Eugene F Fama and Kenneth R French. “Common risk factors in the returns on stocks and bonds”. In: *Journal of Financial Economics* 33.1 (1993), pp. 3–56.
- [30] Eugene F Fama and Kenneth R French. “The Cross-Section of Expected Stock Returns”. In: *The Journal of Finance* 47.2 (1992), pp. 427–465.

- [31] Jianqing Fan, Alex Furger, and Dacheng Xiu. “Incorporating global industrial classification standard into portfolio allocation: A simple factor-based large covariance matrix estimator with high-frequency data”. In: *Journal of Business & Economic Statistics* 34.4 (2016), pp. 489–503.
- [32] Jianqing Fan, Yuan Liao, and Han Liu. “An overview of the estimation of large covariance and precision matrices”. In: *The Econometrics Journal* 19.1 (2016), pp. C1–C32.
- [33] Damien R Farine. “Animal social network inference and permutations for ecologists in R using asnipe”. In: *Methods in Ecology and Evolution* 4.12 (2013), pp. 1187–1194.
- [34] Paweł Fiedor. “Information-theoretic approach to lead-lag effect on financial markets”. In: *The European Physical Journal B* 87.8 (2014), pp. 1–9.
- [35] Michael Goldstein, Amy Kwan, and Richard Philip. “High-frequency trading strategies”. In: *Management Science* 69.8 (2023), pp. 4413–4434.
- [36] Sanford J Grossman and Merton H Miller. “Liquidity and market structure”. In: *The Journal of Finance* 43.3 (1988), pp. 617–633.
- [37] Aric Hagberg, Pieter Swart, and Daniel S Chult. *Exploring network structure, dynamics, and function using NetworkX*. Tech. rep. Los Alamos National Lab.(LANL), Los Alamos, NM (United States), 2008.
- [38] Jarrad Harford and Aditya Kaul. “Correlated order flow: Pervasiveness, sources, and pricing effects”. In: *Journal of Financial and Quantitative Analysis* 40.1 (2005), pp. 29–55.
- [39] Joel Hasbrouck and Duane J Seppi. “Common factors in prices, order flows, and liquidity”. In: *Journal of Financial Economics* 59.3 (2001), pp. 383–411.
- [40] Nicholas Hirschey. “Do high-frequency traders anticipate buying and selling pressure?”. In: *Management Science* 67.6 (2021), pp. 3321–3345.
- [41] Gerard Hoberg and Gordon Phillips. “Text-based network industries and endogenous product differentiation”. In: *Journal of Political Economy* 124.5 (2016), pp. 1423–1465.
- [42] Ruihong Huang and Tomas Polak. “Lobster: Limit order book reconstruction system”. In: *Available at SSRN 1977207* (2011).
- [43] Wei-Qiang Huang, Xin-Tian Zhuang, and Shuang Yao. “A network analysis of the Chinese stock market”. In: *Physica A: Statistical Mechanics and its Applications* 388.14 (2009), pp. 2956–2964.
- [44] Lawrence Hubert and Phipps Arabie. “Comparing partitions”. In: *Journal of Classification* 2.1 (1985), pp. 193–218.
- [45] Ravi Jagannathan and Tongshu Ma. “Risk reduction in large portfolios: Why imposing the wrong constraints helps”. In: *The Journal of Finance* 58.4 (2003), pp. 1651–1683.
- [46] David Krackhardt. “QAP partialling as a test of spuriousness”. In: *Social networks* 9.2 (1987), pp. 171–186.
- [47] David Krackhardt. “Predicting with networks: Nonparametric multiple regression analysis of dyadic data”. In: *Social Networks* 10.4 (1988), pp. 359–381.
- [48] Joseph B Kruskal. “On the shortest spanning subtree of a graph and the traveling salesman problem”. In: *Proceedings of the American Mathematical Society* 7.1 (1956), pp. 48–50.
- [49] L Kullmann, J Kertesz, and RN Mantegna. “Identification of clusters of companies in stock indices via Potts super-paramagnetic transitions”. In: *Physica A: Statistical Mechanics and its Applications* 287.3-4 (2000), pp. 412–419.
- [50] Albert S Kyle. “Continuous auctions and insider trading”. In: *Econometrica: Journal of the Econometric Society* (1985), pp. 1315–1335.

- [51] Olivier Ledoit and Michael Wolf. “A well-conditioned estimator for large-dimensional covariance matrices”. In: *Journal of Multivariate Analysis* 88.2 (2004), pp. 365–411.
- [52] Olivier Ledoit and Michael Wolf. “Improved estimation of the covariance matrix of stock returns with an application to portfolio selection”. In: *Journal of Empirical Finance* 10.5 (2003), pp. 603–621.
- [53] Lily Y Liu, Andrew J Patton, and Kevin Sheppard. “Does anything beat 5-minute RV? A comparison of realized measures across multiple asset classes”. In: *Journal of Econometrics* 187.1 (2015), pp. 293–311.
- [54] Yutong Lu, Gesine Reinert, and Mihai Cucuringu. “Trade co-occurrence, trade flow decomposition, and conditional order imbalance in equity markets”. In: *arXiv preprint arXiv:2209.10334* (2022).
- [55] J MacQueen. “Classification and analysis of multivariate observations”. In: *5th Berkeley Symp. Math. Statist. Probability*. University of California Los Angeles LA USA. 1967, pp. 281–297.
- [56] Rosario N Mantegna. “Hierarchical structure in financial markets”. In: *The European Physical Journal B-Condensed Matter and Complex Systems* 11.1 (1999), pp. 193–197.
- [57] Nathan Mantel. “The detection of disease clustering and a generalized regression approach”. In: *Cancer Research* 27.2_Part_1 (1967), pp. 209–220.
- [58] Harry Markowitz. “Portfolio selection”. In: *The Journal of Finance* 7.1 (1952), pp. 77–91. ISSN: 00221082, 15406261.
- [59] Gautier Marti et al. “A review of two decades of correlations, hierarchies, networks and clustering in financial markets”. In: *Progress in Information Geometry* (2021), pp. 245–274.
- [60] Guido Previde Massara, Tiziana Di Matteo, and Tomaso Aste. “Network filtering for big data: Triangulated maximally filtered graph”. In: *Journal of complex Networks* 5.2 (2016), pp. 161–178.
- [61] Mark McDonald et al. “Detecting a currency’s dominance or dependence using foreign exchange network trees”. In: *Physical Review E* 72.4 (2005), p. 046106.
- [62] Ali Namaki et al. “Network analysis of a financial market based on genuine correlation and threshold method”. In: *Physica A: Statistical Mechanics and its Applications* 390.21-22 (2011), pp. 3835–3841.
- [63] Andrew Y Ng, Michael I Jordan, and Yair Weiss. “On spectral clustering: Analysis and an algorithm”. In: *Advances in Neural Information Processing Systems*. 2002, pp. 849–856.
- [64] Chun-Xiao Nie. “Dynamics of cluster structure in financial correlation matrix”. In: *Chaos, Solitons & Fractals* 104 (2017), pp. 835–840.
- [65] Paolo Pasquariello and Clara Vega. “Strategic cross-trading in the US stock market”. In: *Review of Finance* 19.1 (2015), pp. 229–282.
- [66] Vasiliki Plerou et al. “A random matrix theory approach to financial cross-correlations”. In: *Physica A: Statistical Mechanics and its Applications* 287.3-4 (2000), pp. 374–382.
- [67] Stephen A Ross. “The arbitrage theory of capital asset pricing”. In: *Journal of Economic Theory* 13.3 (1976), pp. 341–360.
- [68] Michael Schneider and Fabrizio Lillo. “Cross-impact and no-dynamic-arbitrage”. In: *Quantitative Finance* 19.1 (2019), pp. 137–154.
- [69] Gustavo Schwenkler and Hannan Zheng. “The network of firms implied by the news”. In: *Boston University Questrom School of Business Research Paper* 3320859 (2019).

- [70] William F Sharpe. “Capital asset prices: A theory of market equilibrium under conditions of risk”. In: *The Journal of Finance* 19.3 (1964), pp. 425–442.
- [71] William F Sharpe. “The sharpe ratio”. In: *Journal of Portfolio Management* 21.1 (1994), pp. 49–58.
- [72] Jianbo Shi and Jitendra Malik. “Normalized cuts and image segmentation”. In: *IEEE Transactions on Pattern Analysis and Machine Intelligence* 22.8 (2000), pp. 888–905.
- [73] Michele Tumminello, Tomaso Aste, et al. “A tool for filtering information in complex systems”. In: *Proceedings of the National Academy of Sciences* 102.30 (2005), pp. 10421–10426.
- [74] Michele Tumminello, Tiziana Di Matteo, et al. “Correlation based networks of equity returns sampled at different time horizons”. In: *The European Physical Journal B* 55 (2007), pp. 209–217.
- [75] Vincent Van Kervel and Albert J Menkveld. “High-frequency trading around large institutional orders”. In: *The Journal of Finance* 74.3 (2019), pp. 1091–1137.
- [76] Ulrike Von Luxburg. “A tutorial on spectral clustering”. In: *Statistics and Computing* 17.4 (2007), pp. 395–416.
- [77] Liyan Yang and Haoxiang Zhu. “Back-running: Seeking and hiding fundamental information in order flows”. In: *The Review of Financial Studies* 33.4 (2020), pp. 1484–1533.
- [78] Yanci Zhang et al. “Company competition graph”. In: *arXiv preprint arXiv:2304.00323* (2023).
- [79] Yichi Zhang et al. “Robust Detection of Lead-Lag Relationships in Lagged Multi-Factor Models”. In: *arXiv preprint arXiv:2305.06704* (2023).

A Spectral Clustering

In this section, we describe the spectral clustering algorithm used to cluster stocks based on the co-trading matrices in Section 4.3.1.

We represent an undirected graph $G = (V, E)$, where $V = \{v_1, v_2, \dots, v_N\}$ is a collection of N vertices which are data points and E is a set of edges, by its (weighted) adjacency matrix $A \in \mathbb{R}^{N \times N}$. The degree matrix of A , denoted as D , is the diagonal matrix with entries

$$D_{ii} = \sum_{j=1, j \neq i}^N A_{ij}.$$

The graph Laplacian L is defined as

$$L = D - A.$$

We use the degree matrix to normalize L , and the normalized version is

$$L_{sym} = D^{-\frac{1}{2}} L D^{-\frac{1}{2}},$$

which contains which contains the information of graph connectivity. Then we perform K-means clustering on the matrix of eigenvectors corresponding to the smallest K eigenvalues of L_{sym} . Here, K is the pre-selected number of clusters. The procedure is summarized in Algorithm 1.

B Random Initialization

Figure 11 plots the average daily ARIs against time. We observe that the values of average daily ARIs are 0.98, 0.93, 0.84 and 0.58, for 11, 15, 20 and 50 clusters respectively. The standard

Algorithm 1 Spectral Clustering

Input: An $N \times N$ similarity matrix A , number of clusters K .

Output: Clusters C_1, C_2, \dots, C_K

- 1: **procedure** SPECTRAL_CLUSTERING(A, K)
 - 2: Compute normalized Laplacian L_{sym}
 - 3: Compute the eigenvectors v_1, v_2, \dots, v_K corresponding to K smallest eigenvalues of L_{sym}
 - 4: Construct matrix $Q \in \mathbb{R}^{N \times K}$ with v_1, v_2, \dots, v_K as columns
 - 5: Form matrix $\tilde{Q} \in \mathbb{R}^{N \times K}$ by normalizing row vectors of Q to norm 1
 - 6: Apply K-means clustering, with K-means++ (Arthur and Vassilvitskii (2006)) for random initialization, to assign rows of \tilde{Q} to clusters C_1, C_2, \dots, C_K
-

deviations of daily ARIs are 0.11, 0.10, 0.07 and 0.03 over the entire period of study. Hence, our clustering analysis on co-trading matrices is robust to random initialization.

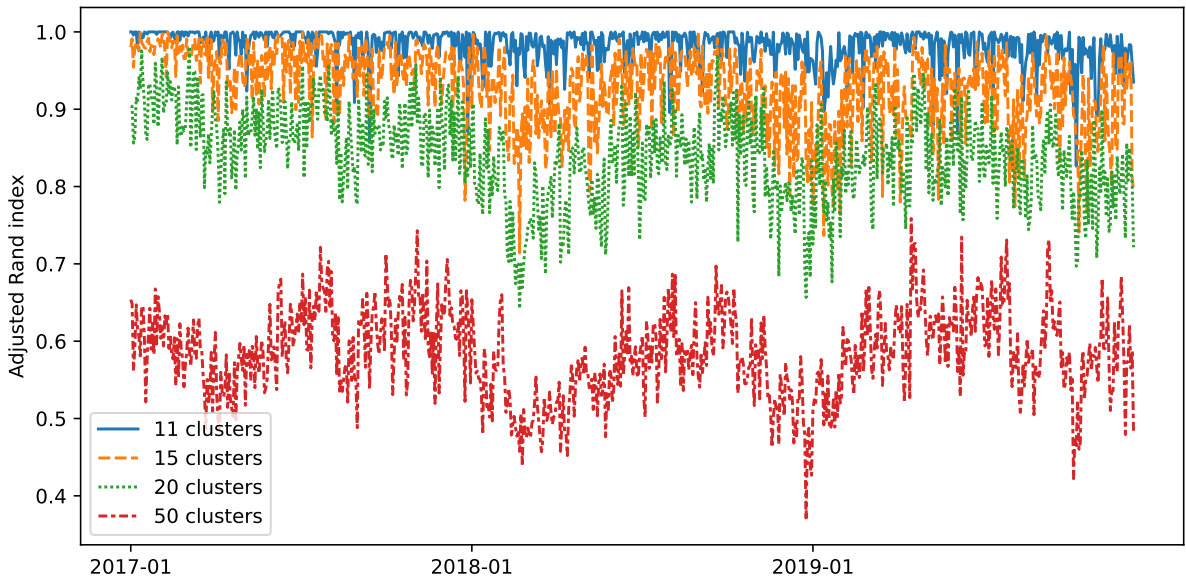


Figure 11: Robustness of applying spectral clustering on daily co-trading networks.

This figure plots the daily means of ARIs between each pair of clusters obtained by running the spectral clustering method 100 times on the same co-trading matrix every day, with different random initialization. Each line corresponds to a value of number of clusters, chosen from 11, 15, 20 and 50.

C Volume Measure

In this section, we define co-trading in terms of volume of trades. As an analogue to Section 3.2, we begin with defining

$$V_{t,j \rightarrow i}^{d^j \rightarrow d^i} = \sum_{x_k \in S_t^{i,d^i}} \sum_{x_l \in \{x_a \in \mathcal{N}_{x_k}^{\delta} \mid s_a = j, d_a = d^j\}} q_l,$$

where S_t^{i,d^i} is the set of all filtered trades and q_l is the size of trade x_l .

Then, the pairwise volume co-trading score between stock i and stock j on day t , using volumes of co-occurred trades for stock i and j with direction d^j and d^i , respectively, is defined

as

$$c_{t,i,j}^{\delta,d^i,d^j} := \frac{V_{t,i \rightarrow j}^{d^i \rightarrow d^j} + V_{t,j \rightarrow i}^{d^j \rightarrow d^i}}{\sqrt{\sum_{x_l \in S_t^{i,d^i}} q_l} \sqrt{\sum_{x_m \in S_t^{j,d^j}} q_m}}.$$

Similarly, incorporating volumes, a pairwise co-occurrence count index is determined by summing up volumes of co-occurred trades of a pair of stocks and normalizing with their total volumes. Finally, we concatenate the pairwise co-trading scores to be the co-trading matrix in volume measure. In line with the main text of the paper, we set δ is set to 500 microseconds.

We repeat the empirical analysis and summarize the results in Table 8. The portfolios based on volume measure underperform those built upon count measure. Furthermore, the volume measured co-trading matrices are less robust than those measured in count of trades.

Table 8: Summary of analysis on volume based co-trading matrices.

We construct volume based daily co-trading matrices from 2017-01-03 to 2019-12-09. Panel A reports the annualized Sharpe ratios of global minimum variance (GMV) portfolios constructed by solving (6) based on different covariance matrices estimates. The ‘Factor’ column specifies the number of latent factors while decomposing the sample covariance matrices. The ‘GICS’ and ‘Count-20’ columns indicate GMV portfolios corresponding to GICS and clustering count based co-trading matrices with 20 clusters as benchmarks. For volume based co-trading matrices, we use 15, 20 and 50 clusters while imposing diagonal block structure on the residual covariance matrices. Additionally, we detect clusters of stocks on volume based co-trading matrices every day with 100 different random seeds for spectral clustering. The predefined number of clusters are 11, 15, 20 and 50. For comparison purpose, we report the statistics for clusters of count based co-trading matrices under. Each value in Panel B is a mean of ARIs between each pair of clusters every day and averaged over all days. Each value in Panel C represents a mean of ARIs between data-driven clusters and GICS sectors each day and averaged over all days.

Panel A: Annualized Sharpe ratios of GMV portfolios.					
Factor	Cluster				
	GICS	Count-20	15	20	50
1	0.45	0.69	0.10	0.65	0.09
3	0.59	1.12	0.36	1.00	0.63
5	0.69	1.23	0.20	0.99	0.80
10	0.97	1.40	0.06	1.07	0.83

Panel B: Average daily ARI among clusters with different initialization.				
Measure	Cluster			
	11	15	20	50
Volume	0.97	0.90	0.80	0.52
Count	0.98	0.93	0.84	0.58

Panel C: Average daily ARI between clusters and GICS sectors.				
Measure	Cluster			
	11	15	20	50
Volume	0.33	0.35	0.33	0.18
Count	0.41	0.43	0.40	0.21